New Fluorinated Thermoplastic Elastomers

CLAUDIO TONELLI,* TANIA TROMBETTA, MASSIMO SCICCHITANO, GIOVANNI SIMEONE, and GIUSEPPE AJROLDI

Ausimont, Centro Ricerca e Sviluppo, Viale Lombardia 20, 20021 Bollate, Milan, Italy

SYNOPSIS

New fluorinated thermoplastic elastomers (FTE) with perfluoropolyether (PFPE) blocks have been synthesized by reacting a fluorinated macrodiol with aromatic diisocyanates in the presence of a solvent, followed by subsequent chain extension with low molecular weight aliphatic or aromatic diols. Tensile properties measurements and dynamical-mechanical analysis (DMA) have been carried out and the relationship between chemical structure and final properties has been determined. These new thermoplastic fluorinated polyurethanes show an elastomeric behavior over a wide temperature range (between −75 and 100°C), thanks to their multiphase morphology consisting of a continuous fluorinated phase with a very low T_g (−120°C) and a dispersed high melting hydrogenated hard phase, as verified by a calorimetric and dynamic-mechanical analysis. At the same time, some of the outstanding properties of fluorinated oligomers, such as chemical inertness and low surface tension, are retained in the final polymers. Thanks to these characteristics this new class of polymeric materials provides new opportunities for the application of thermoprocessable elastomers in advanced technological fields. © 1996 John Wiley & Sons, Inc.

INTRODUCTION

Thermoplastic elastomers (TE) are used more and more in applications previously considered as exclusive domains of conventional crosslinked rubbers. The major advantage of TEs is their ease of processing when compared with the slow and expensive methods needed for vulcanisable rubbers.[1-3] However, thermoplastic elastomers, due to their uncrosslinked structure, cannot match conventional rubber in many aspects. For example they do not have the same high temperature performances as crosslinked rubbers, and their resistance to chemicals and oils is lower. Polyurethanes thermoplastic elastomers (PUTE) have excellent mechanical properties such as abrasion resistance, toughness, and tensile strength. However, their high-temperature performance and chemical resistance are not adequate for many applications, and their low-temperature elasticity is severely limited by the relatively high T_g of the soft segments or their crystallization tendency; this makes conventional polyurethanes unsuitable for temperatures lower than −40°C.

PUTEs are block copolymers in which the soft segments are based on polyester or polyether chains; the polyester types offer some advantages in terms of mechanical properties, high-temperature performance, and thermal stability, while the polyether-based materials have better resistance to hydrolysis and exhibit low-temperature elastomeric behavior (when relatively high molecular weight polyether diols are used).[4-20]

On the basis of these considerations it seems attractive to develop new PUTEs offering the basic advantages of thermoplastic elastomers and exhibiting a lower T_g of the elastomeric block, adequate tensile properties, improved chemical resistance, and a lower surface tension. In principle, these improvements should be achievable by introducing fluorinated blocks into the polymer chains. As a matter of fact, thermoplastic fluoropolymers are commercially succesful thanks to their unique balance of properties, such as low surface energy, low coefficient of friction, nonflammability, low dielectric constant, and high solvent and chemical resistance.[21]

* To whom correspondence should be addressed.

Journal of Applied Polymer Science, Vol. 59, 311–327 (1996)
 CCC 0021-8995/96/020311-17

There are however only few examples of commercially available fluorinated elastomers (FE);[22-25] basically, they are crosslinkable copolymers or terpolymers of vinylidenfluoride or tetrafluoroethylene with few suitable fluorinated comonomers like hexafluoropropene or perfluorovinylethers. Two fluorinated thermoplastic elastomers, where the soft phase is the vinylidene fluoride-hexafluoropropene copolymer, have been recently developed by Daikin,[26] but no examples are found of other kinds of this class of materials. It is believed that the main reason is the very limited availability of suitable fluorinated macromers.

The only fluorinated monomers commercialy available are used primarily as modifiers for conventional PUTE (short-chain fluoroalkene or fluoroether diols). Even if they can be succesfully used to improve the chemical resistance of conventional materials, they do not offer any advantage in terms of the surface properties and temperature service range.[27-32]

The present availability of highly fluorinated building blocks was considered attractive for the synthesis of new polymeric structures offering low-temperature elastomeric behavior, low coefficient of friction, and high chemical resistance. Fluoropoly(oxyalkylene)diol 1 macroglycol was considered a promising candidate to develop thermoplastic elastomers because, in addition to the peculiar properties of fluoropolymers, it is characterized by a very low T_g. This perfluoropolyether (PFPE) macromer is a commercially available building block produced by Ausimont (under the trade name Fomblin ZDOLTX™). It has been developed from a long-term research on the photoxidative polymerization of tetrafluoroethylene and the subsequent thermal and chemical treatment of resulting products[33,34] (Fig. 1).

The presence of functional end groups allows applying conventional polyaddition or polycondensation chemistry to obtain new polymeric materials containing the desired amount of perfluoropolyether chain (PFPE) in the backbone.[35-37] By suitable selection of the type and quantity of starting fluorinated macromer it is possible to obtain polymers with a wide range of PFPE content, varying from a few percent up to 80%. In such a way, polymers that satisfy special application needs can be designed. The aim of this study was to synthesize highly fluorinated thermoplastic polyurethane elastomers, exhibiting the typical outstanding properties of PFPE oligomers and to compare their properties with those of hydrogenated PUTE having the same hard phase.

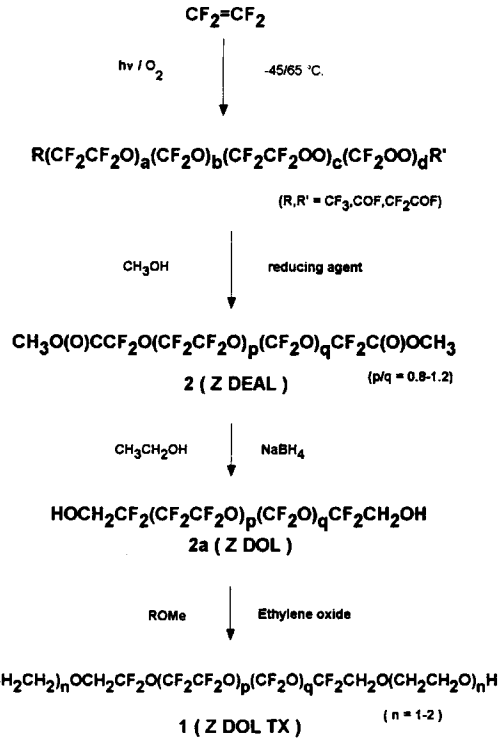

Figure 1 Scheme for the synthesis of Fomblin ZDOL TX.

EXPERIMENTAL

Materials

The following macrodiols were used to synthesize polyurethanes, and their molecular weights were chosen to have nearly the same number of backbone chain atoms n to make easier the comparison among properties.

The fluoropoly(oxyalkylene)diol 1, used in the present work, was a mixture of oligomeric products, consisting of a random distribution of $—CF_2CF_2O—$ (C_2 unit) and $—CF_2O—$ (C_1 unit), end capped by ethoxylated units $—CH_2O(CH_2CH_2O)_nH$, $M_w/M_n < 1.8$, $C_2/C_1 = 0.8–1.2$, $n = 1–2$ and $M_n = 3200–3500$.

Polytetramethylenglycol (PTMEG) was an Aldrich product with a molecular weight of 2000; poly(caprolactone)diol (PCL) was by Interox and has the same molecular weight.

All the macrodiols were dried before use under vacuum at 70–90°C for 2 h.

Some physicochemical properties of the building blocks are collected in Table I; the solubility parameter δ reported in this table is referred to the backbone chain of infinite molecular weight and, in the case of ZDOL TX, the ethoxylated chain ends were

Table I Some Physicochemical Properties of Macrodiols and Hard Segments

		ZDOLTX	PTMEG	PCL	$(MDI\text{-}BDO)_l$	$(MDI\text{-}HQE)_m$
M_n	g/mol	3200–3500	2000	2000	/	/
n	—	100–110	136	122	/	/
δ	$(J/cm^3)^{1/2}$	10.5[39]	17–17.5[38]	19.3[a]	25–26[a]	25–26[a]
T_g	°C	−118/−113	−83,5	−66	/	/
T_m	°C	amorphous	40	40	248/252[a]	269[a]

[a] Calculated from group contributions.

not taken into account; δ values have been found in the literature for PTMEG[38] or were calculated by the group contribution method using the values reported by van Krevelen[38] for PCL and by one of the authors for PFPE.[39]

4,4'Methylenebis(phenyleneisocyanate) (MDI, manufactured by ICI) was purified by filtration at 40°C. 2,2'-(1,4-Phenylenedioxy)diethanol (HQE) was used as received. 1,4-Butandiol (BDO, by Aldrich) was dried under vacuum at 70°C for 2 h. Ethylacetate was distilled and kept under molecular sieves.

Synthesis of Fluorinated Polymers

Fluorinated polyurethanes (FPU) were prepared by a two-step polymerization technique. The synthesis of the prepolymer (first step) was carried out in solvent, while the subsequent chain extension was completed in bulk.

The stoichiometric amount of the diisocyanate was dissolved in ethyl acetate (100 mL of solvent for 100 g of fluorinated macromer). No catalyst was used because of the high reactivity of aromatic isocyanates. The solution was refluxed under nitrogen and the fluorinated macromer was fed dropwise in 3 h. It is believed that this procedure reduces the prepolymer growth giving a more regular polymeric structure after the chain extension. The reaction mixture was kept for another 2 h at the reflux temperature, and the solvent was removed by distillation.

The prepolymer mass was degased under vacuum and the calculated amount of chain extender (BDO or HQE) was added, to give a final NCO/OH ratio of 1.05–1.00, at a temperature of 60–105°C, depending on both the hard phase content and nature of the chain extender. The reaction mass was vigorously stirred for 1–2 min under vacuum. The mass was cast in a mold and placed in a press to complete the polymerization (2 min at 220°C plus 7 h at 130°C).

The reaction kinetics was monitored by IR analysis by observing the decrease of the isocyanate absorption band (2260 cm^{-1}).

Synthesis of the Hydrogenated Polymers

Conventional polyurethanes (HPU) were prepared, for comparison purpose, by a two-step bulk reaction without catalyst. The mold-cast samples were produced with the same thermal cycle used for the preparation of the fluorinated polyurethanes.

Polymer Characterization

All materials were characterized with respect to their hard-phase content, soft segment equivalent weight, and fluorine content. The designations FB and FQ are used to indicate the ZDOLTX/MDI/BDO and ZDOLTX/MDI/HQE systems, respectively. The designations PTB and PCB are used for the PTMEG/MDI/BDO and PCL/MDI/BDO systems, respectively, and, finally, PCQ indicates the PCL/MDI/HQE polymer. The number immediately following the system name refers to the soft-phase equivalent weight, while the number following the dash refers to the hard phase content (percent by volume) calculated on the basis of composition and reagents density.[40] Thus, the sample designated FQ-1600-31 represents an MDI-HQE–based polyurethane containing 1600 eq. wt ZDOLTX and with a hard phase content corresponding to 31% by volume.

All polymers were obtained as slabs (2 or 12 mm thick) by casting, and the samples were conditioned for 2 weeks at room temperature before testing.

Infrared Analysis

The IR measurements were made using a spectrometer IR FT Nicolet 20SX, with a miniature diamont navel cell P/N 2500 for polymeric material analysis.

Differential Scanning Calorimetry

Melting and crystallization were measured according to ASTM D 3417 and D 3418 by means of a Perkin–Elmer DSC 2C Instrument. The scanning range was between 25 and 250°C. By convention, peak temperatures, even when they were broad, were assumed as melting and crystallization temperatures.

The glass transition temperature T_g was determined as midpoint by scans between −160 and 20°C at a scanning speed of 20°C/min; the low temperature range was calibrated with reagent grade *n*-hexane.

Dynamic Mechanical Analysis

Dynamic mechanical properties were measured at a frequency of about 1 Hz by a free oscillation torsion pendulum (Torsionautomat by Brabender) according to ASTM D 2236B. The storage shear modulus G' and the mechanical loss factor Δ have been measured as a function of temperature at 1°C intervals and at a scanning speed of 1°C/min.

Tensile Properties

The stress–strain behavior was determined by means of an Instron dynamometer mod. 1185 at a crosshead speed of 500 mm/min, according to ASTM D 412. Tests at temperatures other than room temperature were carried out in an Instron thermostated oven.

Compression Set

The compression set was measured according to the ASTM D 395 method B on cylindrical specimens (12.5 mm diameter and 12 mm height). The applied compressive strain was 25% and the testing temperatures were 23, 70, and 100°C; the time elapsed under compressive strain was 72 h.

RESULTS AND DISCUSSION

According to the described procedure (see Experimental), two types of thermoplastic fluorinated polyurethane elastomers were synthesized; the composition of these polymers is shown in Table II,

Table II Polymer Compositions

Samples PFPE Based	Equivalent Ratio ZDOLTX/ MDI/CHAIN EXT.[a]	ZDOLTX eq wt	Hard Phase (vol %)	Fluorine Content (wt %)
FB-1750-21	1 : 2 : 1	1750	20.5	51.3
FB-1750-29	1 : 3 : 2	1750	29.1	47.4
FB-1750-33	1 : 3.5 : 2.5	1750	32.6	46.3
FQ-1600-26	1 : 2 : 1	1600	25.5	49.3
FQ-1600-31	1 : 2.5 : 1.5	1600	31.3	46.6
FQ-1600-36	1 : 3 : 2	1600	36.2	44.2
Samples Hydrogenated	**Equivalent Ratio MACROMER/ MDI/CHAIN EXT.[ab]**	**Macromer eq wt**	**Hard phase (vol %)**	**Fluorine Content (wt %)**
PTB-1000-20	1 : 2 : 1	1000	19.8	/
PTB-1000-24	1 : 2.5 : 1.5	1000	24.2	/
PTB-1000-28	1 : 3 : 2	1000	28.1	/
PCB-1000-22	1 : 2 : 1	1000	21.5	/
PCB-1000-30	1 : 3 : 2	1000	30.3	/
PCB-1000-37	1 : 4 : 3	1000	37.3	/
PCB-1000-43	1 : 5 : 4	1000	43.1	/
PCQ-1000-31	1 : 2.5 : 1.5	1000	30.8	/

[a] Chain extender = BDO or HQE.
[b] Macromer = PTMEG or PCL.

Table III Prepolymer Composition

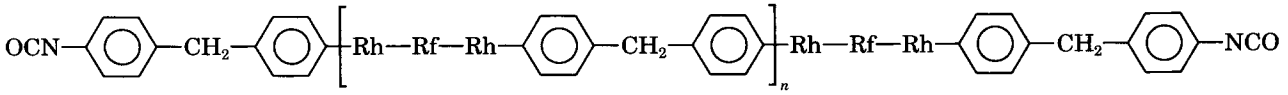

(Rh = —NHC(O)(OCH$_2$CH$_2$)nOCH$_2$—; Rf = —CF$_2$O(CF$_2$CF$_2$O)$_p$(CF$_2$O)$_p$CF$_2$)—

NCO/OH	n
2	1.15
2.5	0.95
3	0.70
3.5	0.55

in which the details of conventional thermoplastic polyurethanes for comparison purposes are also reported.

The prepolymer synthesis was carried out, as described previously, by a procedure that minimizes the prepolymer growth giving a more regular polymeric structure after the chain extension. Nevertheless, depending on the defined stoichiometry, a certain degree of chain extension has always been observed.

Table III reports the relationship between the number of repeating units in the prepolymer and the equivalent ratio (NCO/OH), as determined by end groups titration after extraction of free MDI. From these data it is inferred that, due to the prepolymer growth, part of the MDI couples two soft segments. According to data in the literature[29] related to hydrogenated structure, these MDI units between two soft chains are not phase segregated and, therefore, must be considered as a constituent of the soft phase.

Thermal Behavior

DSC traces for perfluorinated polyurethanes are shown in Figures 2 and 3, and in Figures 4 and 5 for hydrogenated polyurethanes. The observed trends, and the presence of more than one melting peak, are not unusual for polyurethanes; for example, a model relating transitions to microstructure has been put forward by Van Bogart and co-workers.[41,42]

Transitions related to the amorphous and crystalline phases are observed (Table IV), and significant differences are found between the first and second melting.

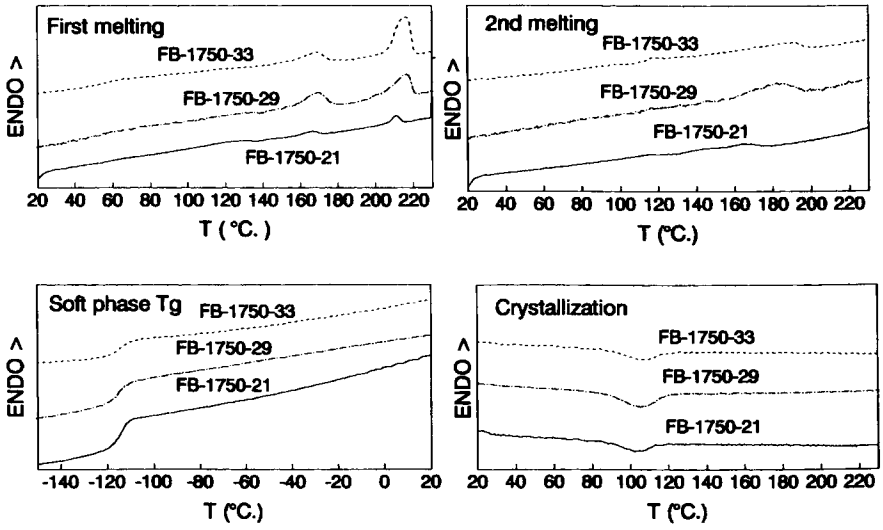

Figure 2 DSC traces for the FB series.

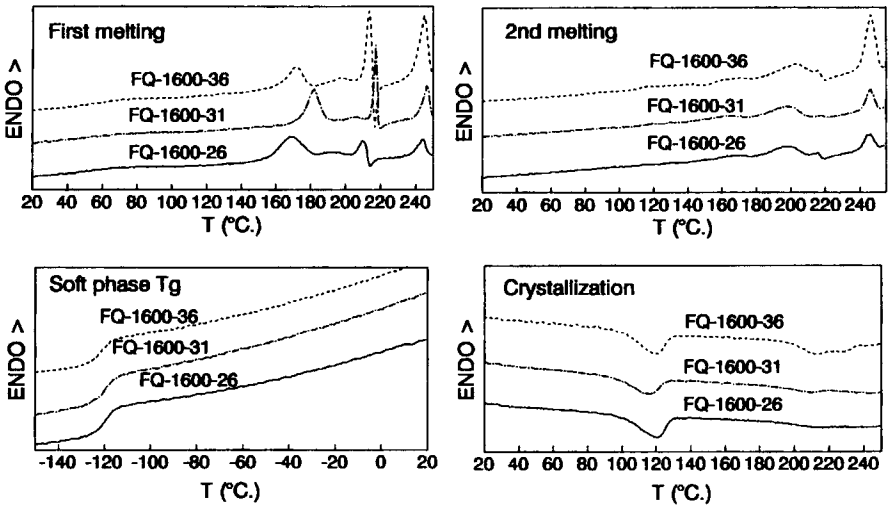

Figure 3 DSC traces for the FQ series.

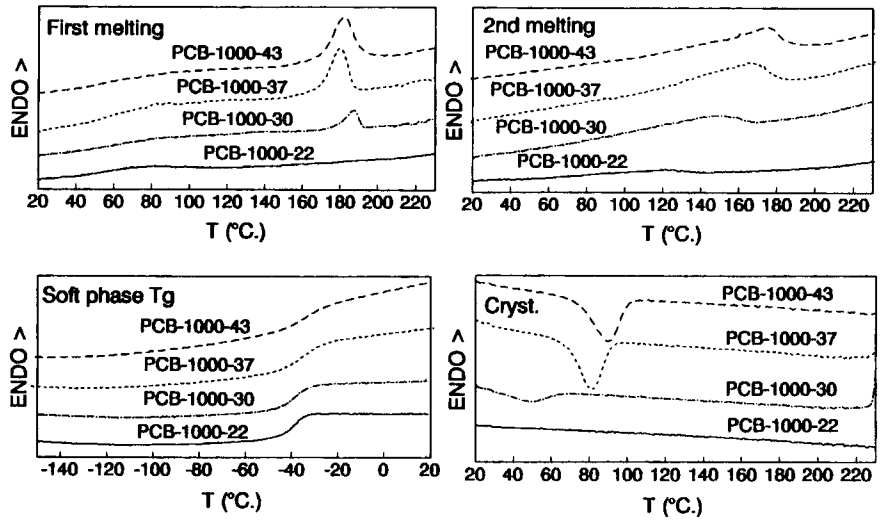

Figure 4 DSC traces for the PCB series.

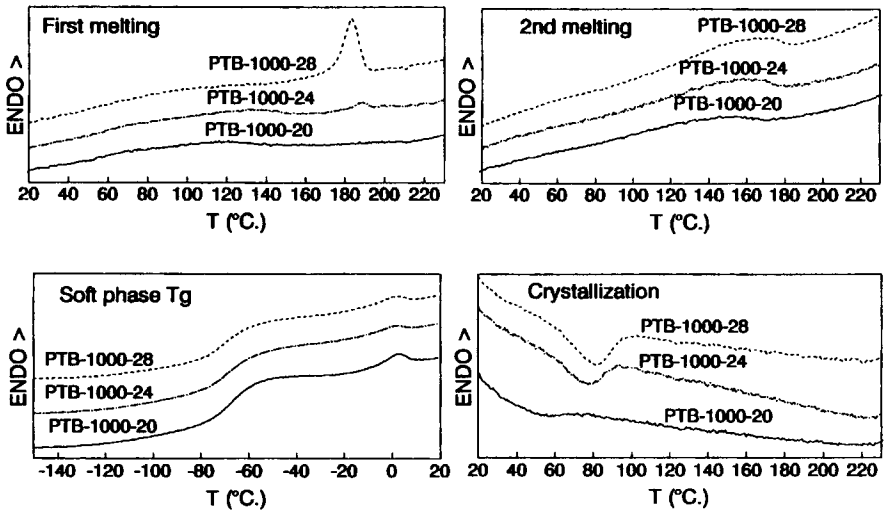

Figure 5 DSC traces for the PTB series.

Table IV DSC Events

Samples	T_g (°C)	Highest T_m (°C)	T_c (°C)	Highest Second Melting T (°C)	ΔH[a] (Cal/g)
FB-1750-21	−120	216	105	170	1.0
FB-1750-29	−120	216	105	181	1.7
FB-1750-33	−120	218	105	186	2.2
PTB-1000-20	−70	108	51	132	2.6
PTB-1000-24	−70	188	77	145	3.5
PTB-1000-28	−70	183	79	155	4.2
FQ-1600-26	−120	245	120–210	245	2.5[b]
FQ-1600-31	−120	247	116–210	246	2.6[b]
FQ-1600-36	−120	245	119–213–227	247	2.9[b]
PCB-1000-22	−40	79	/	/	1.7
PCB-1000-30	−40	187	48	145	1.6
PCB-1000-37	−38	180	81	164	2.7
PCB-1000-43	−38	182	90	174	3.5
PCQ-1000-31	−46	186	74	180	/

[a] Calculated over all the melting peaks.
[b] Underestimated.

The glass transition temperature (T_g) of the soft phase is observed at −120, −70, and −40°C when the soft segment is ZDOL TX, PTMEG, and PCL, respectively. T_g seems to be independent of the hard phase concentration for all the materials investigated, and in the case of perfluorinated materials, also of the chain extender type; this finding suggests that the soft phase is well segregated. Moreover, it is worthy to point out that the observed T_gs are higher than those found in the literature for infinite molecular weight polymers having the same backbone structure. As a matter of fact, T_g = −131°C is reported for Fomblin Z,[43] −84°C for polytetramethyleneoxide,[44] and −60°C for poly-ϵ-caprolactone.[45] Because short chain segments, as those forming the soft phase of PUs, must have a lower T_g if taken alone,[46] i.e., without polar chain ends, one can consider the increase in T_g as the result of two possible causes; the first is the constraint given by chemical links with the hard phase, which certainly reduces the degree of freedom of the soft chain; the second one is a certain degree of compatibility between the soft and the hard phase. This last effect must, however, be highly improbable for perfluorinated PUs when one considers the large difference in solubility parameters (see Table I).

On the other side, the calorimetric behavior of the hard phase is strongly dependent on the structure of both soft and hard phases and on the hard phase volume fraction. For example, FPUs extended with HQE exhibit more complicate DSC traces in both the first and second melting. The crystalline phase MDI-BDO-MDI has a lower melting temperature than the MDI-HQE-MDI rigid phase, which has longer aromatic sequences.

It is now worthy to split the discussion on melting points by considering first the as-cast samples (first melting) and later crystallization and second melting behavior.

First melting data (only the highest T_m was considered) are plotted in Figure 6(a) against the MDI units in the hard phase, as given by stoichiometry; melting temperatures determined by Qin et al.[47] on model compounds of the hard phase are also reported in this figure, because these data represent the maximum melting points for a given polymerization degreee of the hard phase. Horizontal lines drawn in the upper part of the same figure are the limiting values of melting points for infinite molecular weight calculated by group contributions[38] for both MDI-BDO (252°C) and MDI-HQE (269°C) hard phases. While for MDI-HQE no experimental data are available for a comparison, the calculated T_m for MDI-BDO nicely agrees with the experimental value T_m = 248°C reported by Qin.[47] The observed behavior is quite different for each series; melting points of FQ and FB series are apparently insensitive to the hard phase polymerization degree. Because the melting point must increase with this last variable, at least at low polymerization degree, one could reach the conclusion that some dishomogeneous polycondensation had occurred, producing a hard

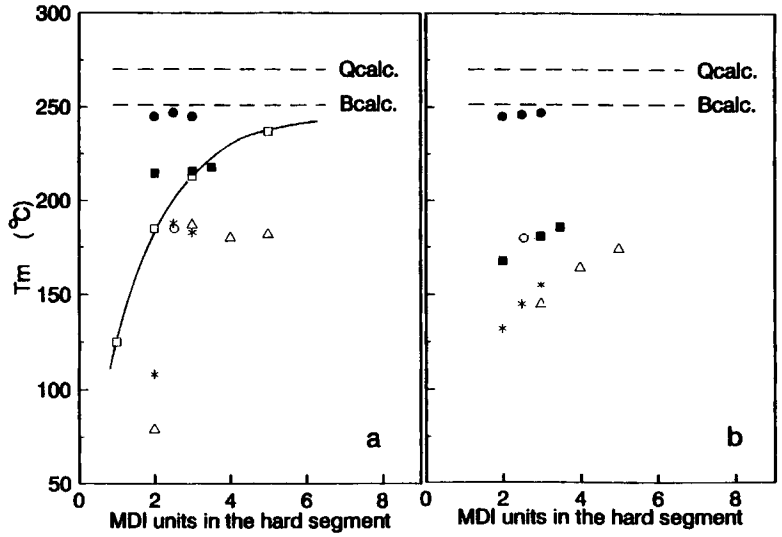

Figure 6 First (a) and second (b) scan melting points as a function of MDI units in the hard segment: (■) FB series, (●) FQ series, (*) PTB series, (△) PCB series, (○) PCQ series, (□) model $(MDI\text{-}BDO)_n$ polymers from ref. 47; horizontal dashed lines show the limiting melting points for MDI-BDO and MDI-HQE of infinite molecular weight calculated by group contributions.

phase with a large polydispersity; thus, hard segments with higher melting points than those expected by stoichiometry are possibly present. As a matter of fact, the corresponding hydrogenated material PCQ-1000-31, with 2.5 MDI groups in the hard segment, has a considerably lower melting point. The hydrogenated PTB and PCB series show, on the other side, an unusual behavior. T_m increases, as expected, with the nominal concentration of MDI units in the hard phase up to a given polymerization degree and then levels off to a nearly constant value. A similar trend with a maximum in the T_m – MDI units curve for MDI = 3 has been also found by Camberlin et al.[48] for fractionated model compounds; these authors attributed the decrease in T_m to a possible chain folding of hard blocks. On the other side, melting points for PTB and PCB polyurethanes (M = 2000 for the soft segments as in the present case) as high as 230–235°C and 211–234°C, respectively, have been reported by Van Bogart and co-workers,[41,49] who prepared their samples by the one-shot technique, which is know to lead to a polidispersity in the hard block dimensions. In the present case, the trend observed is probably due to an artifact induced by annealing after casting carried out at constant temperature, instead that of a constant temperature difference, with respect to the expected melting point; this point will be clearer after the discussion on the second melting.

All the materials, with the only exception of the FQ series, crystallize with some difficulty and undercooling (with reference to the first melting) is generally high (from 60 to 130°C). In the case of FQ series, two crystallization zones are found; the first one exhibits a very low undercooling (20 to 25°C), and the second and more evident one has a very large undercooling (about 125°C). The complexity of DSC traces is observed also in the second melting, so that it seems that two different crystalline structures can possibly coexist. Further work is required to clarify this point.

Finally, the second melting and the difference with the first one are considered. The second melting temperature is plotted against the number of MDI units in Figure 6(b) and as a function of the hard phase content in Figure 7. The FQ series is the only one that does not show any difference between the first and second melting, and a plateau value is reached yet at 26% by volume of the hard phase or two MDI units. A large difference is generally observed for all the other materials, which exhibit lower melting points; the limiting case is given by PCB-1000-22, which, after the first melting, is completely unable to crystallize when cooled. The unusual trend observed before for PTB and PCB series disappears and a regular increase with hard phase concentration is observed; in other words, the higher the hard phase content, bigger and more perfect

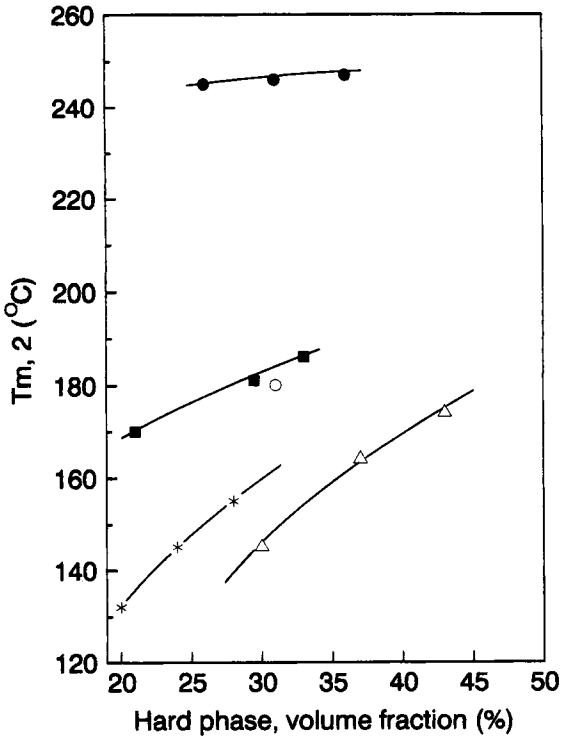

Figure 7 Second scan melting points as a function of the volume fraction of the hard phase. Key as in Figure 6.

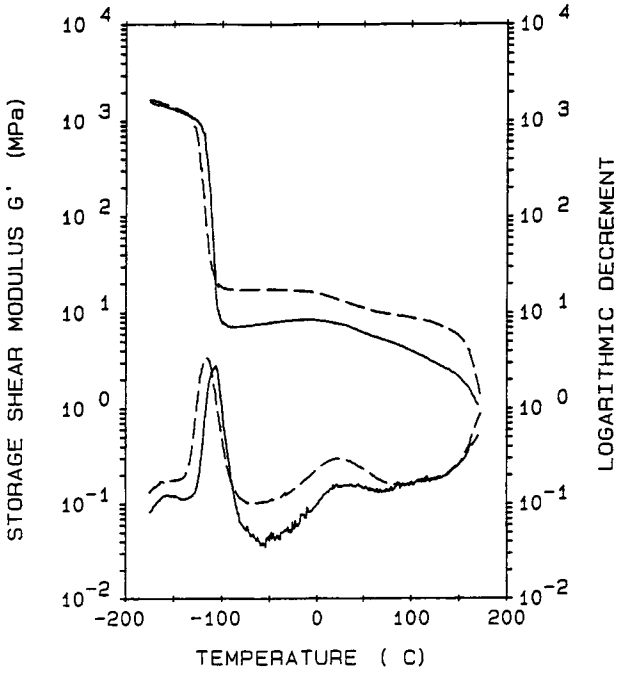

Figure 8 Dynamic-mechanical spectra for FB-1750-29 (continuous line) and FQ-1600-31 (dashed line); the curve of the logarithmic decrement of this last sample has been shifted upward of 0.2 decades for sake of clarity.

crystalline structures are formed. Moreover, a better segregation between phases, i.e., a larger difference in the solubility parameters, improves the perfection of crystallites. As a matter of fact, the best segregation occurs with functionalized Fomblin. If data of PCB and PTB series are considered not as a function of the hard phase concentration as in Figure 7, but as a function of the nominal polymerization degree of the hard phase [Fig. 6(b)], they result to be equivalent.

Dynamic Mechanical Properties

Dynamic mechanical spectra have been determined on as cast materials having a hard phase volume content of about 30%. Spectra are shown in Figures 8 and 9, and the relevant data about transitions are collected in Table V. FPUs show the glass transition of the soft block at temperatures as low as −105 and −115°C; these temperatures are a little higher than those determined by DSC (see Table IV), but in any case, the agreement is sufficiently good. On the left side of the α transition of the soft phase a shoulder or an ill-defined peak is observed at −155°C; its nature is that of a γ relaxation process being related to local motions involving only few in-chain atoms;

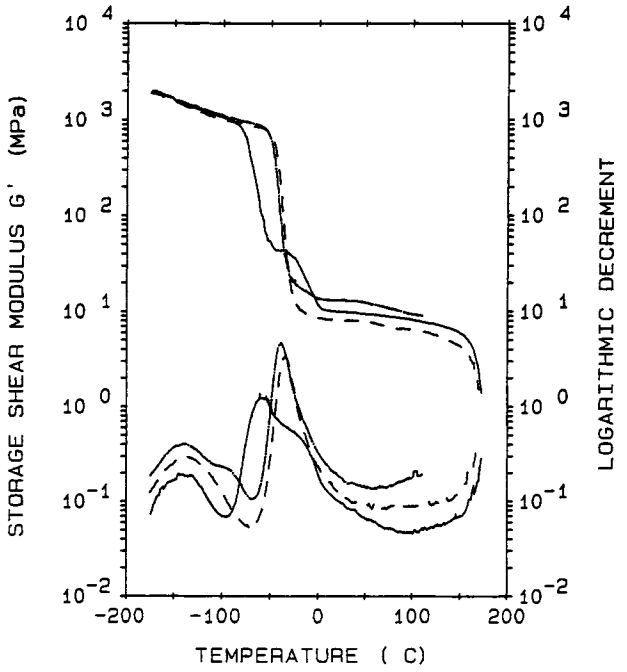

Figure 9 Dynamic-mechanical spectra for PTB-1000-28 (continuous line), PCB-1000-30 (dashed line) and PCQ-1000-31 (— • —); logarithmic decrement curves have been progressively shifted upward of 0.2 decades for sake of clarity.

Table V Relaxation Process by Dynamic Mechanical Spectroscopy

	Soft phase			
Samples	T_γ (°C)	T_β (°C)	T_α (°C)	G', 23°C (MPa)
FB-1750-29	−155	—	−105	7.8
FQ-1750-31	−155	—	−115	14.0
PTB-1000-28	−140	—	−55	10.0
PCB-1000-30	−136	—	−33	8.0
PCQ-1000-31	−138	−95	−38	13.0

such relaxation has been observed for the first time on nonfunctionalized Fomblin fluids.[50]

Peaks in the loss factor related to the T_g of the soft phase are observed at higher temperatures for the hydrogenated materials. The PTMEG based HPU exhibits a composite a maximum with a well-pronounced shoulder on the high temperature side, and the G'-T curve shows in the same temperature range step; such a trend is indicative of crystallization and melting at $T > T_g$ of the soft polyetheric segment. Crystallization and melting phenomena are not found, on the other side, when the soft segment is PCL. All families of HPU exhibit a secondary maximum at low temperatures (γ type), which is related to local motions of few methylene units.[51] A shoulder at about −95°C is also observed for PCQ-1000-31. According to the current literature, it is called β- maximum; it is generally found in polyamides and polyurethanes and is related to solvated hydrogen bonds between contiguous chains; its intensity increases with the adsorbed water content;[51] the absence, or the insufficient intensity, of this maximum in the other HPU simply means that it contained a very small amount, if any, of water.

The two different FPUs both show, at about 20–30°C, a broad relaxation maximum and a decrease in the storage modulus G'; because no evident endotherms are found in DSC traces, it is hypothesized that this transition could be related to the amorphous portion of the hard phase.

It is worthy to observe that the perfluorinated PUs exhibit the best ideal elastomeric behavior in the temperature range below room temperature. As a matter of fact, G' increases with T between −90 and −10°C for FB-1750-29, and remains practically independent of temperature in the same range temperature for FQ-1600-31. On the other hand for HPUs such a behavior is not observed at all or is limited to a very small range. In any case, the general decreasing trend of the G' modulus above room temperature points out that the physical network, due to the hard phase, becomes progressively less stable. Finally, a large drop in modulus occurs at temperatures close to the first melting peak observed in DSC traces for first melting.

The low strain shear modulus data reported in Table V show that the main differences are induced by the hard phase type: PUs based on the MDI-HQE hard phase have moduli significantly higher than those based on MDI-BDO.

Tensile Behavior

Engineering stress–strain curves measured at 23 and 100°C are plotted in Figures 10 and 11, and numerical data are collected in Table VI.

The difference in mechanical properties between FPUs and HPUs is striking, especially at room temperature, where only HPUs exhibit an evident strain hardening; this phenomenon occurs, as expected, at decreasing strain with an increase in the volume fraction of the hard phase. Only in the case of the FB series a very moderate strain hardening can be observed at strains larger than 200%. As it is well known that strain hardening finds its origin in both non-Gaussian behavior at large strains, and in crystallization under strain of the soft segment,[52] it can be reasonably concluded that the moderate strain hardening observed for the FB series is only due to non-Gaussian behavior, because the random copolymeric nature of the soft segment prevents crystallization. Comparison of the stress-strain curves of hydrogenated series at temperatures below (23°C) and above (100°C) the melting point of the soft segments (T_m = 40°C) clearly indicates that crystallization under strain must play a significant role at room temperature.

Another important point is the dependence of the Young modulus E measured at low strain (20%) on the volume fraction of the hard phase and on the structural variables. As shown in Figure 12, the modulus increases with the hard phase concentra-

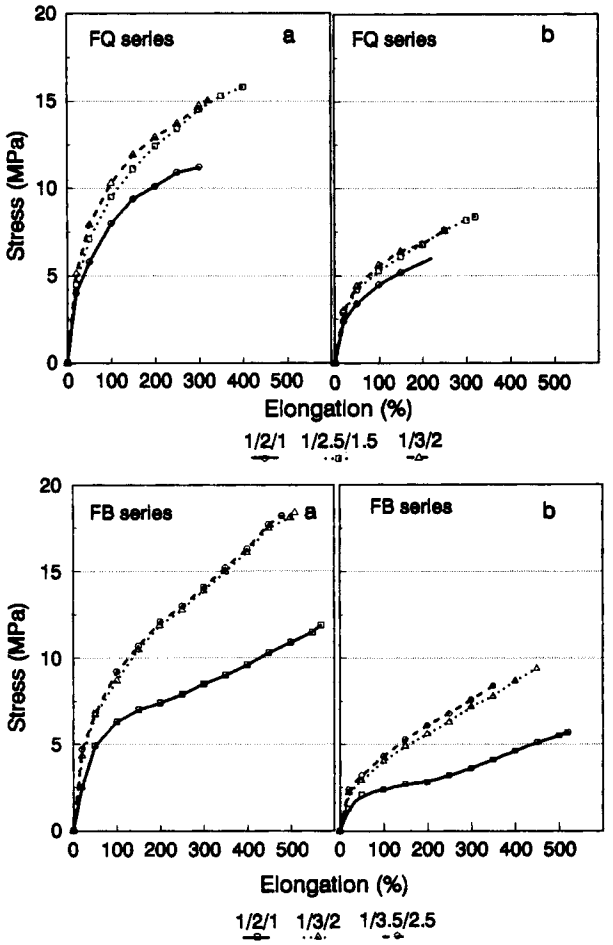

Figure 10 Engineering stress–strain curves at 23 (a) and 100°C (b) for FB and FQ series.

tion, as predicted by theories for two phase polymers.[53]

The modulus is related in principle to the number of crosslinks for unit volume, i.e., to the chain length of the soft segment and to the functionality of crosslinks. ZDOL-TX has a little lower chain length in comparison with the two hydrogenated macrodiols, while the chain flexibility, expressed by the so-called characteristic ratio C_∞ is nearly the same;[39] thus, a little higher modulus must be expected for FPUs at constant crosslink functionality. Moreover, data reported in Figure 12 suggest that a role is also played by the hard phase perfection.

The higher the melting point, the higher the Young modulus; even though it is not perfectly correct to speak about the crosslink functionality for thermoplastic elastomers, one can imagine that the more perfect the crystalline structure, the larger would be the crosslinking efficiency.

The structural stability of the hard phase, which provides the physical crosslinks, can be evaluated by measuring the true secant modulus defined as $\lambda\sigma/(\lambda-1)$, where λ is the draw ratio and σ is the engineering stress, as a function of both temperature and strain.[54] Measurements have been carried out only on a FPU sample, FB-1750-29, between −75 and 100°C; the engineering stress–strain curves are shown in Figure 13. The secant modulus values at $\lambda = 1.2$ and $\lambda = 2$ are plotted in Figure 14 against temperature, together with $3G'$ (shear strain $\gamma < 0.01$) data measured by dynamic-mechanical spectroscopy. It is realized that data are not isochronous but the time scale, however, is not dramatically different (0.4 s for G', 1 and 5 s for $\lambda = 1.2$ and 2, respectively).

The plot clearly shows that the structure is temperature and strain sensitive. At low temperatures the low strain modulus ($3G'$) exhibits a positive temperature coefficient, i.e., a perfectly elastic behavior, but such a behavior is not more observed when the

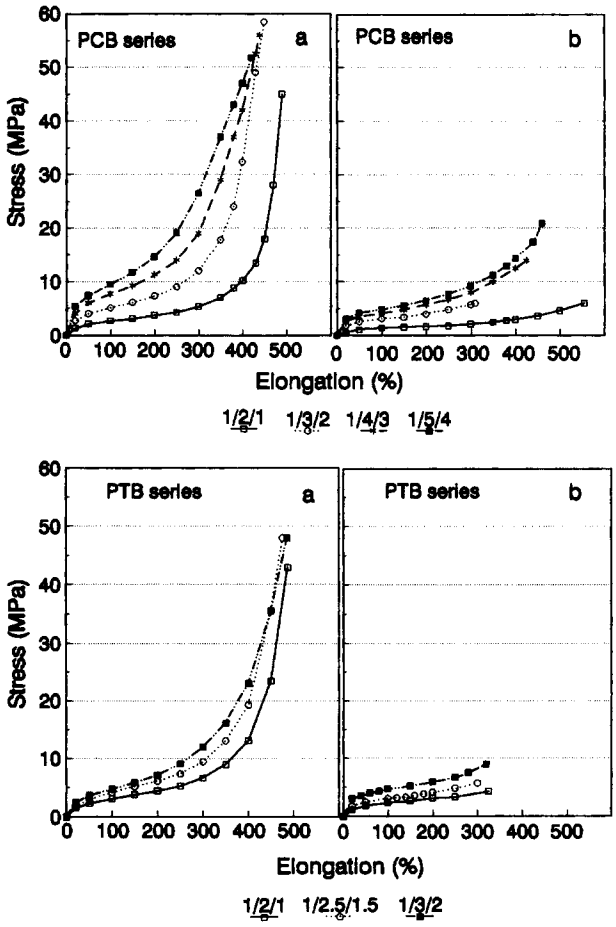

Figure 11 Engineering stress–strain curves at 23 (a) and 100°C (b) for the PTB and PCB series.

Table VI Tensile Properties

Samples PFPE Based	Room Temperature M20% (MPa)	Room Temperature M100% (MPa)	Room Temperature T_b (MPa)	Room Temperature E_b (%)	100°C M20% (MPa)	100°C M100% (MPa)	100°C T_b (MPa)	100°C E_b (%)
FB-1750-21	12.5	6.2	11.5	570	6.7	2.5	5.5	510
FB-1750-29	20.0	8.9	18.0	490	14.0	3.9	9.2	438
FB-1750-33	21.5	9.5	17.7	450	14.5	4.3	8.1	354
FQ-1600-26	22.6	7.8	11.0	290	12.5	4.4	5.8	220
FQ-1600-31	23.8	9.4	15.8	408	14.9	5.2	8.6	330
FQ-1600-36	26.0	10.2	15.0	303	15.5	5.5	7.7	250

Samples Hydrogenated	Room Temperature M20% (MPa)	Room Temperature M100% (MPa)	Room Temperature T_b (MPa)	Room Temperature E_b (%)	100°C M20% (MPa)	100°C M100% (MPa)	100°C T_b (MPa)	100°C E_b (%)
PTB-1000-20	6.5	3.1	42.0	492	5.2	2.2	3.9	320
PTB-1000-24	9.5	4.1	48.3	477	8.9	3.0	5.8	292
PTB-1000-28	13.3	5.5	49.3	480	14.8	4.8	9.1	310
PCB-1000-22	6.5	2.8	45.5	470	2.5	1.5	6.1	558
PCB-1000-30	13.2	5.0	58.0	450	9.0	3.1	6.3	314
PCB-1000-37	20.0	7.6	56.0	435	12.8	4.0	13.2	415
PCB-1000-43	27.2	9.6	52.0	425	15.5	5.0	20.5	456
PCQ-1000-31	18.0	6.4	46.3	565	12.0	4.0	13.4	822

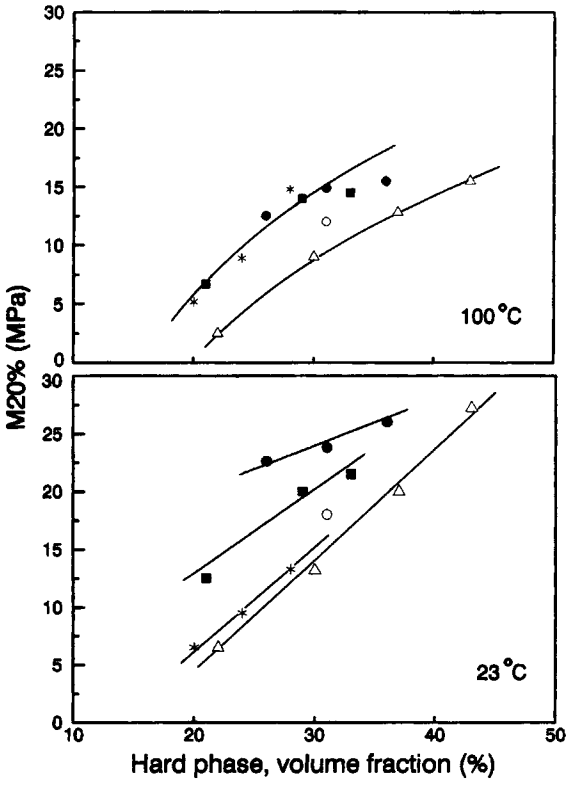

Figure 12 Twenty percent modulus at 23 and 100°C as a function of the hard phase volume fraction. Key as in Figure 6.

strain is increased; the deviation from the ideal behavior increases with strain. It is worthy to observe that the structure stiffens by increasing strain below −25°C, and gradually softens above this temperature.

Data reported by T. L. Smith[54] for PTMEG-MDI-BDO PUs, with M = 2000 for the soft phase, show that the hard phase softens even at temperatures close to the glass transition of the soft phase. A comparison of tensile curves of FB and PTB materials at a constant hard phase volume fraction and at about the same reduced temperature $T - T_g$ (Fig. 15) shows the role played by the different macrodiols; it is believed that the strong incompatibility between the Fomblin Z DOL TX and the MDI-BDO blocks brings about a better separation of the hard phase and a different and stiffer hard phase.

Tensile data measured as a function of temperature, shown in Figure 13 for an FB material, and the comparison of tensile curves reported in Figure 15 point out the FPUs exhibit at low temperature very good strength and elongation, which are similar or superior to those of HPUs at room temperature; at this last temperature, FPUs exhibit lower strength, but they show a more gradual decrease in strength with temperature in comparison to HPUs; the experimental data show, indeed, that the loss in strength between 23 and 100°C is lower for FPUs.

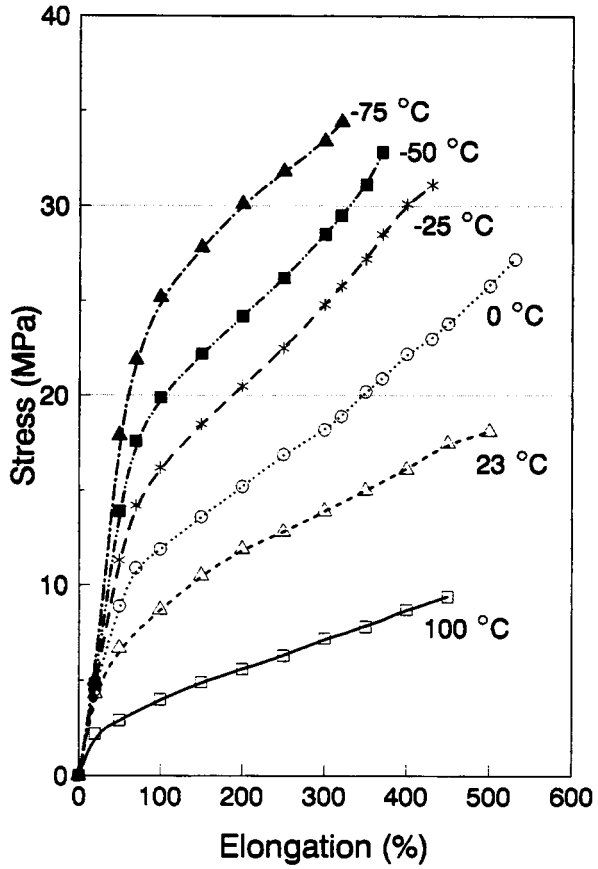

Figure 13 Engineering stress–strain curves for FB-1750-29 measured at several temperatures.

In conclusion, FPUs exhibit elastomeric properties over a larger temperature range, because of the lower T_g of the soft segment.

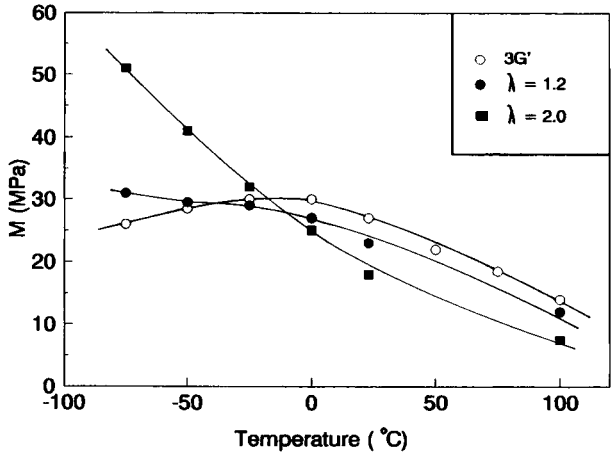

Figure 14 Modulus of FB-1750-29 as a function of both applied strain and temperature: (○) $3G'$, (●) $\lambda = 1.2$, (■) $\lambda = 2.0$.

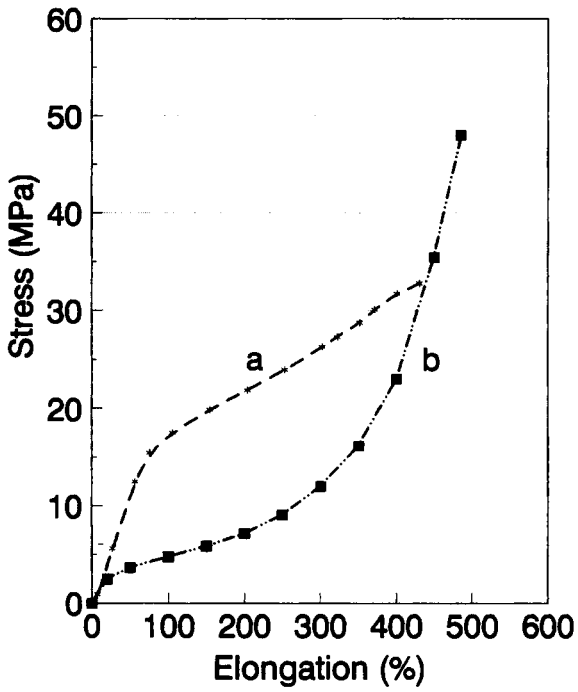

Figure 15 Comparison of the engineering stress–strain curves at about the same reduced temperature $T - T_g$ for: (a) FB-1750-29 ($T = -25$°C), (b) PTB-1000-28 ($T = 23$°C).

The Compression Set

The compression set data also give important information about the elastomeric recovery of the materials as a function of structure, temperature, and time. Table VII summarizes these data for fluorinated polyurethanes as a function of testing temperature; two hydrogenated materials have been added for comparison.

The compression set performance is mainly dependent on the structure of the hard phase; the higher the rigidity and the local yield stress of the hard segment, the lower is the residual deformation

Table VII Compression Set (%)

	Temperature (°C)		
Samples	23	70	100
FB-1750-21	19	45	81
FB-1750-29	34	79	94
FB-1750-33	23	67	97
FQ-1750-26	8	21	54
FQ-1750-31	11	22	49
FQ-1750-36	12	30	58
PCB-1000-43	/	61	78
PCQ-1000-31	8	20	/

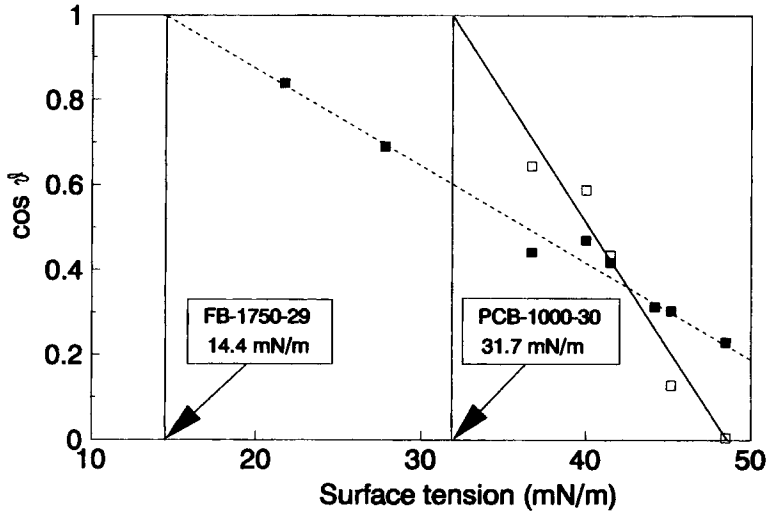

Figure 16 Extrapolation of surface tension of FPU (FB-1750-29) and HPU (PCB-1000-30) by the contact angle method.

after aging at a given temperature; FPUs and the HPU sample based on the MDI-HQE hard phase show the lowest values even at high temperature when compared to the series based on MDI-BDO hard segment. The structure of the macrodiols seems to be irrelevant in determining the compression set; the hard phase volume fraction plays the role of a second-order effect; these conclusions hold, of course, only within the boundaries of the compositional range studied.

Finally, the difference between the two series increases with the temperature.

Surface Properties

Finally, surface tension determinations, obtained through contact angle measurements with a series of solvents having different surface tension (Fig. 16 and Table VIII), have confirmed our previous findings[40] that the surface of these new FPUs consists essentially of perfluorinated chains. The critical gamma values are, in fact, close to the typical values of perfluoropolyether chains (15 mN/m).

Chemical Resistance

The presence of fluorinated domains in the polymeric microstructure and especially on the free surfaces of specimens or molded items significantly improves the chemical resistance, particularly with respect to aggressive polar solvents. Swelling phenomena and deterioration of tensile properties are, in fact, significantly reduced in comparison with conventional polymers. Table IX shows the results of chemical aging tests and demonstrates that the fluorinated polymers (FB and FQ series) have a su-

Table VIII Contact Angle Measurements

Liquid	γ_{LC} (mN/m)	PCB-1000-30		FB-1750-29	
		$\bar{\vartheta}$	cos $\bar{\vartheta}$	$\bar{\vartheta}$	cos $\bar{\vartheta}$
Ethylene glycol	48.5	90.4	−0.0065	76.7	0.230
1,4-Butanediol	45.2	82.6	0.128	72.3	0.304
DMSO	44.2	71.7	0.315	71.7	0.314
Methylformamide	41.5	64.2	0.435	65.3	0.418
2-Chloroethanol	40.0	53.9	0.589	61.9	0.471
Pluronic 10R5	36.7	49.8	0.645	63.8	0.442
Acetic acid	27.8	/	/	46.3	0.691
2-propanol	21.7	/	/	32.9	0.840

Table IX Chemical Aging (23°C, 72 h)

Samples	Volume	Property Change (%)		
		Weight	Hardness	Tensile Strength
FB-1750-21				
H_2SO_4 (3% sol.)	0.3	0.2	2.6	−24
NaOH (1% sol.)	0.2	0.1	1.2	6
H_2O	0.3	0.1	1.2	16
Ethanol	6.8	3.2	−7.7	−52
THF	350	150	n.d.[a]	n.d.
Ethyl acetate	24.9	13.1	n.a.[b]	n.a.
MEK	31.4	14.8	n.a.	n.a.
DMF	89.9	49.8	n.a.	n.a.
FQ-1600-26				
H_2SO_4 (3% sol.)	0.1	0.1	0.0	4
NaOH (1% sol.)	0.1	0.1	−1.2	0
H_2O	0.2	0.1	2.4	0
Ethanol	6.4	3.1	−6.0	−30
THF	37.0	19.0	−19.3	−64
Ethyl acetate	20.6	10.9	n.a.	n.a.
MEK	21.6	10.3	n.a.	n.a.
DMF	87.3	48.7	n.a.	n.a.
PTB-1000-20				
H_2SO_4 (3% sol.)	1.3	1.2	−2.9	−18
NaOH (1% sol.)	1.3	1.3	−4.4	−32
H_2O	1.3	1.3	−8.7	−18
Ethanol	101.0	75.6	−62.3	−79
THF		Completely dissolved		
Ethyl acetate	87.9	73.5	n.a.	n.a.
MEK	113.1	84.6	n.a.	n.a.
DMF		Completely destroyed		
PCQ-1000-31				
H_2SO_4 (3% sol.)	n.a.	n.a.	n.a.	n.a.
NaOH (1% sol.)	n.a.	n.a.	n.a.	n.a.
H_2O	n.a.	n.a.	n.a.	n.a.
Ethanol	n.a.	n.a.	n.a.	n.a.
THF	329.9	252.8	n.d	n.d
Ethyl acetate	90.1	69.8	n.a.	n.a.
MEK	114.4	79.3	n.a.	n.a.
DMF		Completely dissolved		

[a] Not determinable.
[b] Not available.

perior chemical resistance than the equivalent hydrogenated polymers (PTB series). Acids, bases, and water do not affect the physical and mechanical properties of fluorinated materials, although in this respect the hydrogenated material also show a fairly good resistance to these chemicals. The superior performance of fluorinated materials is particularly evident when the resistance to polar solvents is measured.

Although these solvents reduce the properties of PTB or completely dissolve the hydrogenated polymer in some cases, the fluorinated polymers only undergo some swelling. The extent of swelling phenomena not only depends on the nature of the chemicals, but also on the structure of the hard phase. A superior performance is, indeed, obtained with polymers in which the hard phase is constituted by long sequences of aromatic rings (FQ series).

CONCLUDING REMARKS

Taking all these characteristics into considerations it is clear that these new FPUs show a better performance than conventional PU, thanks to their capability of preserving a large part of outstanding properties of perfluoropolyether segment, such as low glass transition, chemical inertness, and low surface tension.

New high technological applications, until now precluded for conventional PU, can be proposed, therefore, for this new class of polymers.

The authors wish to thank Prof. A. Turturro of the Genova University for providing surface tension data, and Miss Rosalba Fiore and Mr. Luca Bondanza for their help in the synthesis of the polymers. The assistance of Mr. G. Castiglioni, Mr. M. Fumagalli, and Dr. A. Staccione, who supervised most of the mechanical tests and thermal analyses, is also gratefully acknowledged.

REFERENCES

1. J. W. C. Van Bogart, P. E. Gibson, and S. L. Cooper, *Rubber Chem. Technol.*, **54,** 963 (1981).
2. R. Bonart, *Polymer,* **20,** 1389 (1979).
3. J. W. C. Van Bogart, A. Lilaonitkul, and S. L. Cooper, *Adv. Chem. Series,* **176,** 3 (1979).
4. J. W. C. Van Bogart, P. E. Gibson, and S. L. Cooper, *J. Polym. Sci., Polym. Phys. Ed.,* **21,** 65 (1983).
5. R. W. Seymour and S. L. Cooper, *Macromolecules,* **6,** 48 (1973).
6. P. Wright and A. P. C. Cumming, *Solid Polyurethane Elastomers,* Mc Laren and Sons Ltd., London, 1969
7. R. J. Athey, *Rubber Age,* **96,** 705 (1965.
8. C. S. Schollenberger and F. D. Stewart, *J. Elastoplast.,* **3,** 28 (1971).
9. Z.T. Ossefort and F.B. Testroet, *Rubber Chem. Technol.*, **39**, 1308 (1966).
10. G. B. Guise and G. C. Smith, *J. Macromol. Sci. Chem.,* **A14,** 213 (1980).
11. T. M. Chapman, *J. Polym. Sci., Polym. Chem. Ed.,* **27,** 1993 (1989).
12. O. Bayer, *Rubber Chem. Technol.,* **23,** 812 (1950).
13. J. Wright, *Eur. Rubber J.,* **159**(3), 13 (1977).
14. J. H. Saunders and K. C. Frisch, *Polyurethanes Chemistry and Technology,* Part I, John Wiley, New York, 1962
15. K. Schauerte, in *Polyurethane Handbook,* G. Oertel, Ed., Hanser, Munich, 1985, p. 50
16. T. M. Chapman, D. M. Rakiewicz–Nemeth, J. Swestock, and R. Benrashid, *J. Polym. Sci., Polym. Chem. Ed.,* **28,** 1473 (1990).
17. T. M. Chapman, and R. Benrashid, *J. Polym. Sci., Polym. Chem. Ed.,* **28,** 3685 (1990).
18. K. C. Frisch, S. L. Reegen, and L. P. Rumao, *Advances in Urethane Science and Technology,* Vol. 1, Chapt. 3, Technomic, Stanford, 1971.
19. M. Spirkova, M. Kubin, and K. Dusek, *J. Macromol. Sci. Chem.,* **A27,** 509 (1990).
20. T. B. Chapman, *J. Polym. Sci., Polym. Chem. Ed.,* **27,** 1993 (1989).
21. M. M. Lynn and A. T. Worm, in *Encyclopedia of Polymer Science and Engineering,* Vol. 7, J. I. Kroschwitz, Ed., Wiley Interscience, New York, 1987, p. 256
22. D. Apotheker, J. B. Finlay, P. J. Krusic, and A. L. Logothetis, *Rubber Chem. Technol.,* **55,** 1004 (1982).
23. M. Oka and M. Tatemoto, in *Contemporary Topics in Polymer Science,* Vol. 4, Plenum Press, New York, 1984, p. 763
24. Silastic℠, Dow, Fluorosilicone Rubbers Technical Bulletin.
25. D. P. Tate, *J. Polym. Sci., Polym. Symp.,* **48,** 33 (1974).
26. Dai-el℠ Thermoplastic, Daikin, Technical Bulletin.
27. T. M. Keller, *J. Polym. Sci., Polym. Chem. Ed.,* **23,** 2557 (1985).
28. S. C. Yoon and B. D. Ratner, *Macromolecules,* **19,** 1068 (1986).
29. S. C. Yoon and B. D. Ratner, *Macromolecules,* **21,** 2392 (1988).
30. S. C. Yoon and B. D. Ratner, *Macromolecules,* **21,** 2401 (1988).
31. S. C. Yoon, Y. K. Sung, and B. D. Ratner, *Macromolecules,* **23,** 4351 (1990).
32. T. Takakura, M. Kato, and M. Yamabe, *Makromol. Chem.,* **191,** 625 (1990).
33. D. Sianesi, A. Pasetti, R. Fontanelli, G. C. Bernardi, and G. Caporiccio, *Chim. Ind. (Milan),* **5,** 208 (1973).
34. R. A. Mitsch and J. La Mar Zollinger, U.S. Pat. 4094911 (1978).
35. G. Caporiccio, E. Strepparola, G. Bargigia, G. Novaira. and G. Peveri, *Makromol. Chem.,* **184,** 935 (1983).
36. R. A. Mitsch and J. La Mar Zollinger, U.S. Pat. 3810874 (1974).
37. R. A. Mitsch and J. La Mar Zollinger, U.S. Pat. 3972856 (1976).
38. D.W. van Krevelen, *Properties of Polymers,* Elsevier, Amsterdam, 1976.
39. G. Marchionni, G. Ajroldi, M. C. Righetti, and G. Pezzin, *Macromolecules,* **26,** 1751 (1993).
40. C. Tonelli, T. Trombetta, M. Scicchitano, and G. Castiglioni, *J. Appl. Polym. Sci.,* **57,** 1031 (1995).
41. T. R. Hesketh, J. W. C. Van Bogart, and S. L. Cooper, *Polym. Eng. Sci.,* **20,** 190 (1980).
42. J. W. C. Van Bogart, D. A. Bluemke, and S. L. Cooper, *Polymer,* **22,** 1428 (1980).
43. G. Marchionni, G. Ajroldi, P. Cinquina, E. Tampellini, and G. Pezzin, *Polym. Eng. Sci.,* **10,** 829 (1990).
44. U. Gaur and B. Wunderlich, *J. Phys. Chem. Ref. Data,* **10,** 1001 (1981).
45. C. G. Seefried, Jr. and J. V. Koleske, *J. Polym. Sci., Polym. Phys. Ed.,* **13,** 851 (1974).
46. R. F. Boyer, *Macromolecules,* **7,** 142 (1974).
47. Zh. Y. Qin, C. W. Macosko, and S. T. Wellinghof, *Macromolecules,* **18,** 553 (1985).

48. Y. Camberlin, J. Pascault, M. Letoffe, and P. Claudy, *J. Polym. Sci., Polym. Chem. Ed.*, **20,** 383 (1982).
49. J. W. C. Van Bogart, A. Lilaonitkul, L. E. Lerner, and S. L. Cooper, *J. Macromol. Sci. Phys.*, **B17,** 267 (1980).
50. G. Ajroldi, G. Marchionni, M. Fumagalli, and G. Pezzin, *Plast. Rubber Compos. Proc. Appl.*, **17,** 307 (1992).
51. N. G. McCrum, B. E. Read, and G. Williams, *Anelastic and Dielectric Effects in Polymeric Solids*, John Wiley, London, 1967.
52. L. R. G. Treloar, *The Physics of Rubber Elasticity*, Clarendon Press, Oxford, 1949.
53. L. E. Nielsen, *Mechanical Properties of Polymers and Composites*, Chapt. 7, Vol. 2, M. E. Dekker, New York, 1974.
54. T. L. Smith, *Polym. Eng. Sci.*, **17,** 129 (1977).

Received April 27, 1995
Accepted July 7, 1995